Study of the Orientation and the Degree of Exfoliation of Nanoparticles in Poly(ethylene–vinyl acetate) Nanocomposites

F. Cser, S. N. Bhattacharya

Rheology and Materials Processing Centre, School of Civil and Chemical Engineering, RMIT University, Melbourne, Victoria 3000, Australia

Received 15 July 2002; accepted 17 March 2003

ABSTRACT: Nanocomposites formed from organically modified montmorillonite and poly(ethylene-*co*-vinyl acetate) were studied by X-ray diffraction techniques. Wide- and small-angle X-ray scattering intensities (SAXS and WAXS) were recorded by transmission mode on test bars cut from compression-molded plaques tilted by different angles with respect to the plane of the plaque. The height of the Bragg peaks characteristic of intercalated particles reduced to the baseline at tilt angles greater than 30°. Guinier analysis of the SAXS characteristic of particle scattering showed a radius of gyration of 0.69 nm and the scattering intensity was slightly dependent on the tilt angle. Recording of WAXS in the usual (i.e., in reflective) mode enhanced the effect of the structural features of the surface area and showed much higher degree of intercalation and particle size of the scattering particles than that in transmission mode. © 2003 Wiley Periodicals, Inc. J Appl Polym Sci 90: 3026–3031, 2003

Key words: nanocomposites; intercalation; exfoliation; WAXS; dispersions

INTRODUCTION

Polymeric nanocomposites are now in the forefront of polymeric research. Scientifically the nanocomposites formed from layered silicate as nanofillers constitute the most important class of these composites. Their physical properties depend greatly on the degree of dispersion of the nanofillers.

When the lamellae are fully dispersed in the matrix polymer, exfoliated structures are formed. Here the polymeric matrix separates the individual galleries of the clay mineral, although they are not characterized by a regular, periodic arrangement. In exfoliated structures the inorganic lamellae covered by the surface-modifying organic layer form particles with different electron densities with respect to that of the matrix polymer; therefore they can be detected from the lowest angle fraction of the X-ray diffraction scattering curve [small-angle X-ray diffraction (SAXS)].

The other type is the intercalated structure, where the polymeric material forms only a thin, usually only a monomolecular, layer between the galleries of the clay mineral and the clay particles swollen by the polymer are dispersed in the remaining polymeric matrix. The galleries form a periodic structure and their periodicity can be measured by X-ray diffraction (XRD) technique. Bragg peaks in the wide-angle X-ray diffraction scattering (WAXS) curve with greater Bragg periods with respect to the organoclay are the indicators of the presence of intercalated structures.

XRD is widely used in the representation of nanostructures of polymeric nanocomposites.[1–7] Usually the details of the experimental conditions, except the type of the X-ray, are not reported. Most XRD intensity curves are recorded by counting detectors, but there are also some studies that use the film technique. The latter was used to show distribution of the orientation of nanoparticles within injection-molded polyamide 6 test bars. By use of a microfocusing source, a rapid change in the orientation of particles as a function of the depth of the sample was detected.[6]

In most of the studies reported in the literature only WAXS intensities are given.[1–5] The aim of the XRD results is to show the presence or the absence of Bragg diffraction peaks characteristic of intercalation; that is, only the layer periods measured on the nanocomposites are compared to those of the organoclay alone. If the layer period of the nanocomposite is greater than that of the organoclay used to prepare the nanocomposite, the system is declared to be intercalated. If the layer period is not measurable, the nanocomposite is declared to be exfoliated.

Lincoln et al.[7] used simultaneous WAXS and SAXS data to study the structural features of nylon-6 nanocomposites using synchrotron radiation. From the absence of the original Bragg diffraction peak of the organoclay they concluded that the structure was exfoliated. From the SAXS data they calculated a lamel-

Correspondence to: F. Cser (ferenc.cser@rmit.edu.au).

Journal of Applied Polymer Science, Vol. 90, 3026–3031 (2003)

lar particle thickness of 2.2 nm using Guinier approximation. However, the SAXS data also showed a subperiodicity of 40 nm, similar to that obtained from TEM micrographs. Here exfoliated individual lamellae formed a semiperiodic system because it would be an extremely intercalated nanocomposite.

Recently a conventional XRD test was carried out in the reflection mode, as shown in Figure 1(A). Here the collimated X-ray [*i*, i.e., incident beam in Fig. 1(A)] hits the surface of a plate and the scattering intensities [*s*, i.e., scattering beam in Fig. 1(A)] are collected mainly from the surface area of the material indicated by *V* in Figure 1(A). The surface effect is particularly enhanced in the scattering intensities at low scattering angles and when the sample contains elements from the second row or higher, that is, when the absorption of the X-ray restricts the scattering to a small depth of the sample. This is the case of nanocomposites where there are 5–10% of aluminosilicates in the material.

Originally, XRD analysis was carried out in transmission mode when the scattering intensities were recorded on films. The so-called Buerger camera used for this technique was generally equipped by a rotating engine, and the sample was rotated during the scattering test. The effect of a possible orientation of the crystallites can be eliminated by rotating the sample during the exposure by X-ray. Figure 1(B) shows the diffracting geometry of the transmission mode using electronic intensity measurement. The effect of the orientation of the structural elements, however, cannot be eliminated by this technique because the sample has a fixed position with respect to the radiation and its plane is tilted by half of the diffraction angle to the direction of the X-ray beam; however, the dominating effect of a surface layer can be eliminated in this way. Through the use of different tilt angles of the sample with respect to the direction of the X-ray beam the orientation of the structural elements with respect to a specific direction of the sample (e.g., direction of the injection molding, axes of film blowing, plane of the compression molding, etc.) can be tested.

Another way to test the orientation of the structural element in polymeric test bars is to use two-dimensional detectors for intensity measurement. The micro-XRD technique in transmission mode was used by Worley et al.[6] to show the orientation of nanolamellae

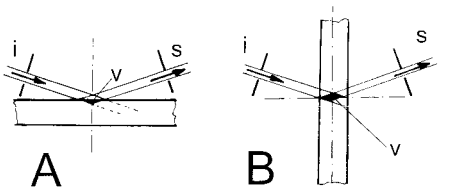

Figure 1 Geometry of the recording modes of the X-ray scattering. (A) reflective mode; (B) transmission mode.

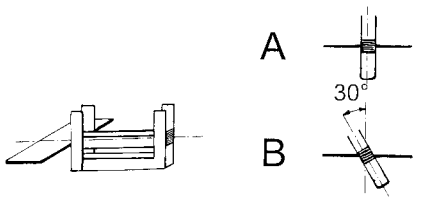

Figure 2 Sample holder for transmission-mode recordings. (A) for 0, 45, and 90° tilt angles, respectively; (B) for 15, 30, 60, and 75° tilt angles, respectively. For the test using 15, 45, and 75° tilt angles, respectively, rods with ends trimmed by 45° are used.

in polyamide 6. The intensities were recorded by film method to obtain two-dimensional intensity function.

Preliminary XRD studies on nanocomposites in our laboratory showed great differences in the WAXS and SAXS intensities recorded in different modes (reflection and transmission). Special sample holders were therefore constructed and used to record XRD intensities at different tilt angles of the sample in transmission mode. The sample holders are shown in Figure 2. The results of the test are given and discussed in this work.

EXPERIMENTAL

Materials

Poly(ethylene-*co*-vinyl acetate)s (EVA) of film-blowing grade with 28 and 9% of vinyl acetate content were used. The samples were marked as EVA28 and EVA09.

Sample preparation

Sodium-modified bentonite with cation exchange capacity of 85 mequiv/100 g of clay (obtained from UNIMA-Australia Ltd.) was reacted in water with cetyl-trimethyl-ammonium bromide obtained from Sigma Aldrich, Ltd. at 40°C for 2 h. One mol ammonium salt was used for 1 mol of sodium in sodium bentonite. The precipitated organoclay was filtered after 24 h of sedimentation time, washed with demineralized water, dried, and milled to obtain a powder with a particle size of less than 40 μm.

Preparation of EVA28 nanocomposites

Initial mixing of 5% of organically modified bentonite to EVA was carried out in a Banbury twin-screw compounder at 80°C using 70 rpm for 40 min. The product was pelletized and compression molded at 110°C for 15 min to form 3-mm-thick sheets. The molding time was 5 min. Rods of 3-mm width and 20-mm length were cut from the plaques and used for XRD testing.

Preparation of EVA09 nanocomposites

Cetyl-modified clay of 5 wt % was mixed with EVA in a Haake (Bersdorff, Germany) Rheocord 90 internal mixer. The set temperature of the mixer was 95°C. Mixing was done at 70 rpm for 15 min. Then the nanocomposite was compression molded to sheets at 120°C for 10 min.

XRD intensities were recorded by a Philips (The Netherlands) X-ray generator using 30-kV accelerating voltage and 30-mA current. Ni-filtered Cu–K_α radiation was used to record intensities from $2\theta = 1.5$ to 45° recording range. The intensities were scaled to a common scale using the amorphous scattering portion of the EVA (2θ = 17–19 and 30–45°). Samples were positioned in a perpendicular sample holder to record data from the sample tilted by 0 and 90°, positioned in the sample holder tilted by 30° to record data tilted by 30 and 60°, respectively. Finally, the rod was trimmed by 45° at its ends to record data tilted by 45° using sample holder A shown in Figure 2. The measurement of the tilt angle using this recording technique is approximate; however, it is useful to show the effect of the orientation of the structural elements on the nanocomposites.

The scattering intensities were recorded by computer and modified by subtracting the background scattering measured by an empty sample holder to provide information at the small-angle part of the scattering intensities. Quinier analysis is generally carried out on small-angle scattering after a couple of corrections (e.g., desmearing).[8] Because our valuable records started at 1.5° scattering angle, only the background was removed and no other correction was employed. Because the smallest angle portions of the scattering curves are absent, Quinier analyses can provide results only on thickness data of the exfoliated lamellae; no superperiodicity or structure can be detected in this way. This technique, however, can show some characteristics of the degree of exfoliation; thus it can provide some semiquantitative data about the structures and there is no need for the more laborious procedure of SAXS data collection.

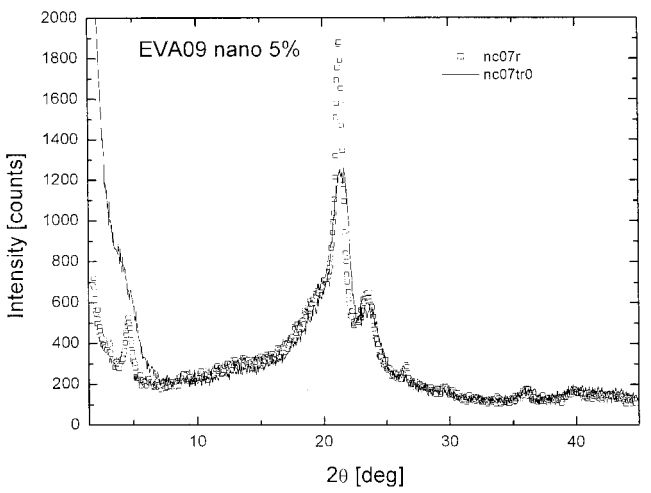

Figure 3 WAXS intensities of EVA09 5% nanocomposite recorded by different methods.

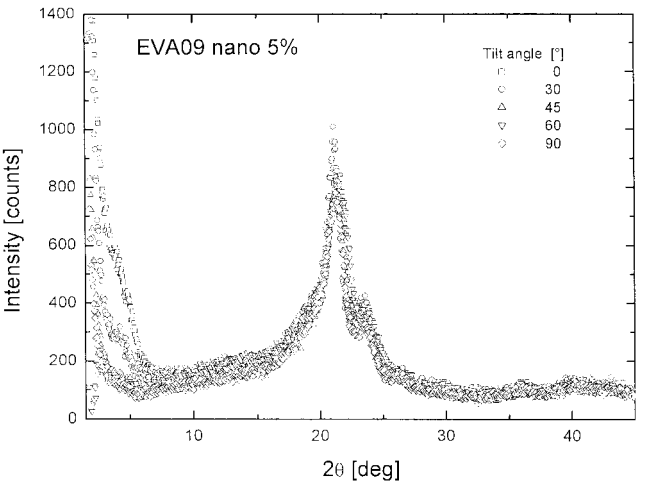

Figure 4 WAXS intensities of EVA09 5% nanocomposite as the function of the tilt angle.

RESULTS AND DISCUSSION

Figure 3 shows the scattering intensities of EVA09 nanocomposites as a function of the scattering angle and of the recording technique of the sample. The tilt angle was 0°. A sharp Bragg peak can be seen on the record at $2\theta = 4.6°$, taken by reflective technique corresponding to a repetition period of 1.92 nm. This peak reflects an intercalated structure with relatively high particle size along the periodicity (from the line width, using a Scherrer equation, a particle size of 45 nm was estimated). The organo-bentonite has a repetition periodicity of 1.96 nm. The recording carried out by transmission technique shows a broad peak with approximate periodicity of 2.2-nm peak, and it is superimposed on a strong primary peak. The crystalline peak characteristic of polyethylene (PE) is more intense in the reflective recording mode than in the transmission mode.

Figure 3 is a confirmation of the structural differences that characterize the surface area with respect to the bulk of the compression-molded plaque. The nanocomposite shows dominantly intercalated structure in reflective mode with a Bragg peak of 1.93 nm periodicity. Because the organoclay used for preparation of this material has a long spacing of 1.96 nm, the composite seems to be a nonreacted system. The transmission mode recording, however, shows a reacted system, with 2.2 nm of periodicity, and much smaller particle size of the swollen organo-bentonite.

Figure 4 shows the scattering intensities of EVA09

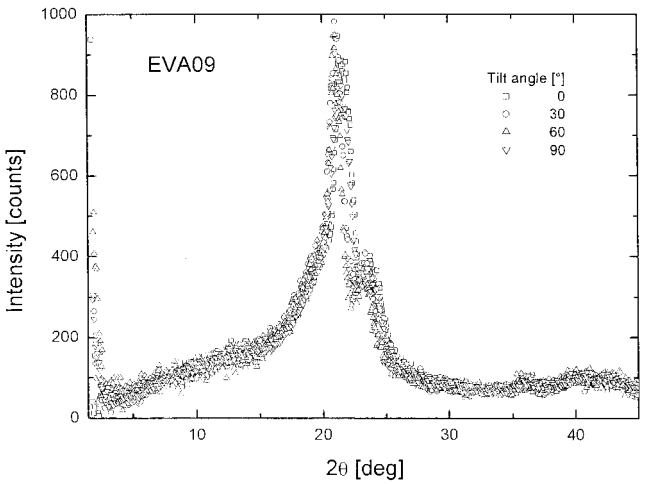

Figure 5 WAXS intensities of EVA09 matrix polymer as the function of the tilt angle.

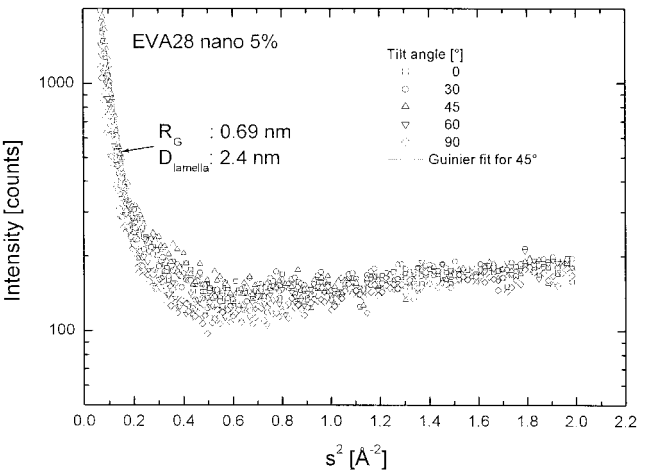

Figure 7 Guinier representation of the SAXS intensities of the EVA29 5% nanocomposites.

nanocomposite recorded in transmission mode at different tilt angles. The intensity of the peak characteristic of intercalated structures is strongly reduced in the curve recorded at 30° of tilt angle and it is absent in all of the other records. The small-angle portion of the scattering can be observed at higher tilt angles but with reduced scattering intensities with respect of the 0° tilt angle records.

Figure 5 shows the scattering intensities of the matrix polymer. When the records are superimposed on each other, there is no detectable dependency of the scattering intensities on the tilt angle. This corresponds to the expectations that EVA09 itself is supposed to be a randomly oriented semicrystalline material.

Figure 6 shows the scattering intensities of EVA28 5% nanocomposites recorded at different tilt angles. The nanocomposite does not show any Bragg peak characteristic of intercalated structures. It shows, however, strong scattering intensities toward the zero angles. The smallest angle intensities are shown according to a Guinier representation in Figure 7. There is a slight dependency of the intensities on the tilt angles. The sample with 45° of tilt angle showed the highest scattering intensities at small-angle range. All samples with different tilt angles show very similar dependency of the intensities toward the zero angle, meaning that they show very similar particle size of the scattering particles. The radius of gyration calculated using a Quinier formula resulted in 0.69 nm, which corresponds to 2.4 nm lamellar thickness in the case of high aspect ratio lamellar scattering particles. This value is close to the expected lamellar thickness of individual organically modified galleries of bentonite as well as the periodicity detected by WAXS scattering (1.96 nm).

Figure 8 shows the scattering intensities of the ref-

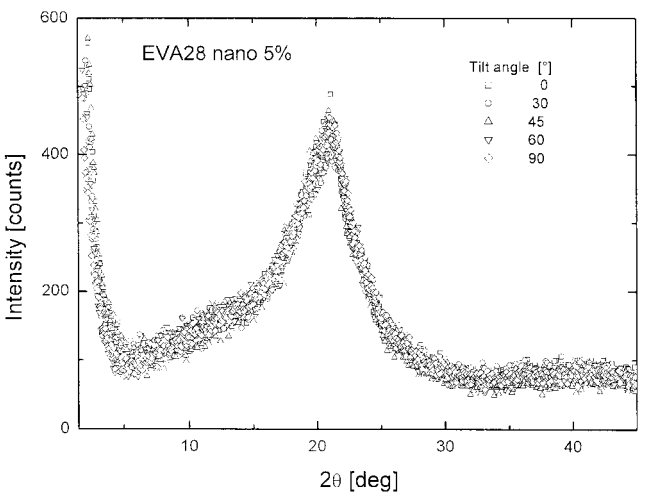

Figure 6 WAXS intensities of EVA28 5% nanocomposites as the function of the tilt angle.

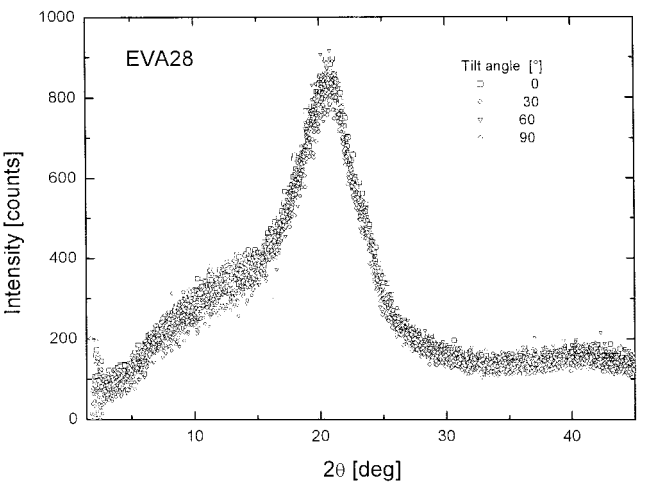

Figure 8 Scattering intensities of EVA28 polymer as the function of the tilt angle.

erence polymer, EVA28. There is no dependency of the scattering intensities on the tilt angle. This polymer has a very low crystallinity; therefore the broad double peak in the 10–28° range of the scattering angle shows a nearly completely amorphous nature.

Currently, the generally accepted XRD testing technique is the reflective mode of data collection. As Figure 3 shows it clearly, polymeric nanocomposites show different WAXS and SAXS intensities according to the method of the data collection. SAXS intensities are generally collected in transmission mode. It is highly important to estimate the ratio of the amount of the two structural forms within the nanocomposite. The combined WAXS and SAXS intensity data collection technique can result in comprehensive data of the degree of exfoliation.

The intensity data shown in Figures 3–8 were therefore corrected to the background. The most important parts of the SAXS intensities are absent from the intensity data, and thus the lag of the SAXS intensities can be approached only by using Guinier's approximation, given by the following equation:

$$I(s) = I^0 \exp\left(- \frac{1}{3} R_g^2 s^2 \right) \tag{1}$$

Here I is the scattering intensity as a function of the scattering vector [$s = 4\pi \sin(\theta)/\lambda$], R_g is the radius of gyration of the scattering particles, and λ is the wavelength of the X-ray beam. This formula is generally used in the differential form at the smallest diffraction angle to calculate the dimension of the possible largest particles. If we turn the differential form to the intensities we have a Gaussian type of function with the center of the peak at a zero diffraction angle (i.e., at $s \rightarrow 0$). Because the XRD intensities are the convolution of those of different structural features, the primary peak can be accepted, as would be the sum of the peaks generated by particles with different radii of gyration:

$$I(s) = \sum_i I_i(s) = \sum_i I_i^0 \exp\left(- \frac{1}{3} R_{g,i}^2 s^2 \right) \tag{2}$$

The Bragg peaks at the WAXS intensities are also approached by Gaussian shape. The following function can therefore be fitted to the experimental data composed of n components:

$$I(s) = \sum_i^n A_i \exp[- B_i (C_i - s)^2] \tag{3}$$

where $i = 1$ represents the SAXS scattering component; thus $C_1 = 0$.

Figure 9 shows the least square (LQ) fit of the function shown as eq. (3) with $n = 2$ to the smallest angle part of the measured intensities for EVA09 nanocomposite recorded at a tilt angle of 0°. Figure 10 shows the LQ fit for intensity data recorded at a tilt angle of 30°. The parameters of the excellent fits of the data ($r^2 \sim 0.99$) are given in Table I.

The Bragg diffraction peak has the same s values in both tilt angles. The line widths of the Bragg peaks are broad, indicating the small particle size of the intercalated organoclay. The Bragg periodicities are 2.29 and 2.32 nm for the two tilt angles, respectively. They differ within the expected precision of the measurement. The line widths of the two lines correspond to 172 and 213 nm of particle size for the lamellae.

The data obtained from the fit can be transformed to the ratio of the exfoliated versus intercalated phases using the ratio of the area under the SAXS peak to the sum of those of the Bragg peaks. In our case the

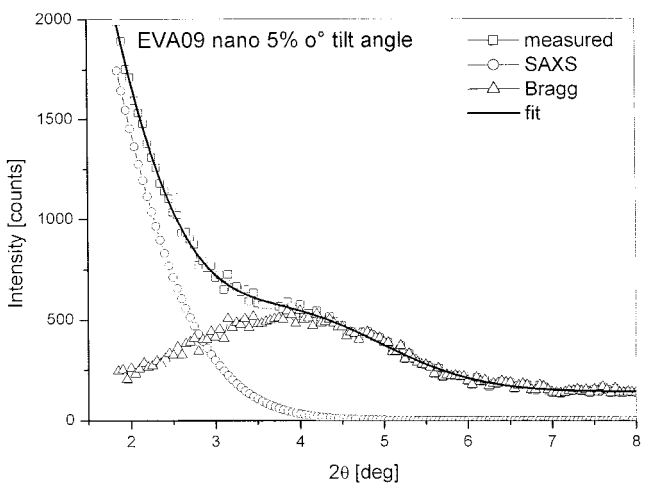

Figure 9 SAXS and Bragg components of EVA09 nanocomposite at 0° tilt angle produced by LSQ fit.

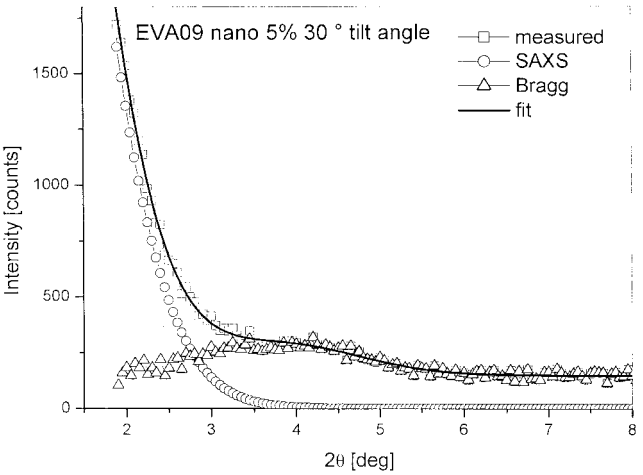

Figure 10 SAXS and Bragg components of EVA09 nanocomposite at 30° tilt angle produced by LSQ fit.

TABLE I
Parameters of the Best Fit for EVA09 Nano 5% Samples and the Corresponding Physical Data

Tilt angle	A	B	C	I_0	D (nm)	R_g/L (nm)
SAXS component						
0	5160	63	—	5160	—	2.1
30	8450	91	—	8450	—	2.5
Bragg component						
0	375	74	0.2742		2.29	172
30	140	111	0.2713		2.32	213

EVA09 nano 5% sample showed ratios 11.8 and 49.5 for the two tilt angles, respectively. If we assume that the exfoliated and intercalated portions of the organoclay do not depend on the tilt angle of the test, the figures mean that we measure a greater exfoliated portion with respect to the intercalated one in the 30° tilt angle test. This means that the exfoliated portion of the nano particles is less oriented than the intercalated portion, which is highly oriented. This corresponds to that observed for the EVA28 nano 5% sample.

CONCLUSIONS

The preceding study showed that the XRD scattering curves of nanocomposites highly depend on the data collection techniques. The generally used method is to collect data in the reflection mode. This leads to misinterpretations concerning structural features. The transmission method is used generally in both SAXS and Synchrotron devices for WAXS data collection. Because even the compression-molded samples show highly oriented features, the normally accepted techniques to test with beam direction perpendicular to the sample surface do not show the proper structural state of the polymeric nanocomposites.

The small-angle part of the XRD scattering curves can be deconvoluted according to particle and reciprocal lattice scattering, respectively, and the ratio of the exfoliated to intercalated structures may be computed after suitable calibration. A relative change attributed to different parameters of the preparation, however, can be computed without calibration.

References

1. Hoffmann, J. G. B.; Dietrich, C.; Thomann, R.; Friedrich, C.; Mulhaupt, R. Macromol Rapid Commun 2000, 21, 57.
2. Shen, Z.; Simon, G. P.; Cheng, Y.-B. J Aust Ceram Soc 1998, 34, 1.
3. Jalcin, B.; Cakmak, M. ANTEC 2001, SPE 2208–2212, 2001.
4. Wang, H.; Zeng, C.; Svoboda, P.; Lee, L. J. ANTEC 2001, SPE 2203–2207, 2001.
5. Lincoln, D. M.; Vaia, R. A.; Wang, Z.-G.; Hsiao, B. S. Polymer 2001, 42, 1621.
6. Worley, D. C.; Akkapeddi, M. K.; Socci, E. P. ANTEC 2001 SPE 2120–2124, 2001.
7. Saujanya, C.; Padalkar, A. S.; Radkharishnan, S. Polymer 2001, 42, 2255.
8. Glatter, O.; Kratky, O. Small Angle X-ray Scattering; Academic Press: London, 1982.